

# Performance of a metal hydride device for simultaneous heat transformation and refrigeration

M. Ajay, M.P. Maiya and S. Srinivasa Murthy\*

Refrigeration and Air Conditioning Laboratory, Department of Mechanical Engineering, Indian Institute of Technology Madras, Chennai 600 036, India

## Abstract

An analysis of a metal hydride-based system for simultaneous heat transformation and refrigeration is presented. A six-reactor configuration comprising of three different hydriding alloys has been considered taking account of the coupled heat and mass transfer in the reactors. The influence of parameters like cycle time and operating temperatures has been studied. It was found that the cycle time plays an important role and has to be selected judiciously for specified output. Among the various operating temperatures it was observed that the heat source and heat rejection temperatures have significant influence on the system performance.

*Keywords:* metal hydride; heat and mass transfer; refrigeration; heat transformation; six reactor configuration; cycle time

\*Corresponding author:  
ssmurthy@iitm.ac.in

Received 23 February 2009; revised 15 April 2009; accepted 16 April 2009

## 1 INTRODUCTION

Recently, metal hydrides have generated significant interest owing to their wide range of applicability in various fields like hydrogen storage, heating and cooling, etc. The simplest metal hydride-based cooling systems are based on single stage cycles. However, these devices have low coefficient of performance (COP) and low specific thermal output when compared with conventional thermal energy conversion systems.

Many works have been published on the heat and mass transfer aspects of metal hydride heat pumps and refrigerators. Ram Gopal and Srinivasa Murthy [1] studied the performance of a metal hydride refrigerator based on ZrMnFe/MmNi<sub>4.5</sub>Al<sub>0.5</sub> and brought out the importance of bed thickness and effective thermal conductivity in the design of practical systems. They concluded that each bed thickness corresponds to an optimal effective thermal conductivity beyond which the performance of the system does not improve. The effects of cooling time, regeneration time and different temperatures on the performance of a metal hydride chiller were investigated by Kang and Kuznetsov [2]. The optimum periods for cooling and regeneration were found based on COP and cooling capacity.

Ahmed and Srinivasa Murthy [3] reported a novel three-alloy application which gives simultaneous heat transformation and cooling output in a complete cycle. The schematic of the working of the three-alloy system is shown in Figure 1. The cycle works at

four temperature levels  $T_{tr}$ ,  $T_s$ ,  $T_{rej}$  and  $T_{ref}$  where  $T_{tr}$  is the temperature at which transformed heat at a higher temperature is obtained,  $T_s$  the temperature at which heat input is given,  $T_{rej}$  heat rejection temperature and  $T_{ref}$  the temperature at which cooling is obtained. The performance of the system was studied for the effects of operating temperatures, reaction rate and cycle times. This idealized thermodynamic study was performed under uniform temperature and concentration conditions in the reactors.

The reaction of metal hydride with hydrogen is dynamic and is influenced by the heat and mass transfer rates. In order to obtain a thorough understanding of the system behaviour, a detailed study involving the heat and mass transfer aspects of these systems is required. The present work is intended towards the simulation of the working of the metal hydride-based device incorporating the heat and mass transfer aspects so that the prediction comes closer to the actual working conditions. The heat and mass transfer study incorporates the reactor configuration, temperature and concentration variations, and heat interactions with heat transfer fluids.

## 2 DESCRIPTION OF THE THREE-ALLOY DEVICE

The schematic of the device consisting of three alloys is shown in Figure 1. It operates at four temperature levels. Here, a heat

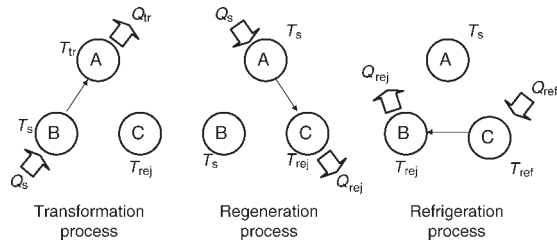


Figure 1. Schematic of the working of a three-alloy system.

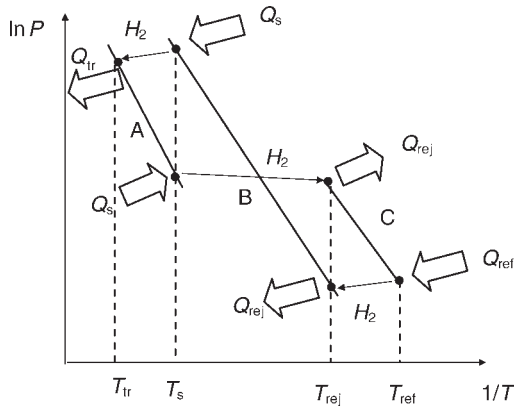


Figure 2. Working of a three-alloy system in a van't Hoff chart.

transformation alloy A (an alloy which can deliver heat output at a desired high temperature) works intermittently between heat transformation temperature and a heat source temperature. Similarly, a refrigeration alloy C works between refrigeration temperature and heat rejection temperature. The regeneration alloy B is coupled with the transformation and refrigeration alloys in the heat transformation and refrigeration processes, respectively.

Figure 2 shows the working cycle on a van't Hoff's chart. Initially, A and C are in dehydrogenated condition at the heat transformation and heat rejection temperatures, respectively. The regeneration alloy B is rich in hydrogen at the heat source temperature. A and B are connected for the heat transformation process. Because of the heat input at the regeneration

alloy B, hydrogen gets desorbed and is absorbed simultaneously by alloy A releasing the heat at high temperature. Once this transformation process is completed, the regeneration and refrigeration alloys (A and C) are connected for the regeneration process. Heat is supplied to the transformation alloy (A) to transfer hydrogen to the refrigeration alloy C. The latter rejects the heat to the ambient during this regeneration process. Then alloys B and C are connected. Cooling load is absorbed by C at low temperature and the released hydrogen is absorbed by alloy B rejecting heat to the ambient. This completes the cycle.

It can be seen that the cycle working on the three-alloy system yields heat transformation as well as refrigeration only intermittently. In order to get continuous outputs one more set of these three alloys are coupled in six-reactor configuration as shown in Figure 3. Here, all the three processes can occur at the same time as depicted in the figure. Another benefit of this configuration is that the cycle completes in just two steps as against three steps in basic three-alloy system. Thus theoretically, it should give 50% more yield in terms of output. Hence this configuration is used for the current study.

### 3 MATERIAL SELECTION AND PROPERTIES

The primary criterion for the selection of the three alloys A, B and C is that in order to facilitate hydrogen transfer equilibrium pressure of the alloy, which is desorbing hydrogen, should be more than that of the alloy, which is absorbing hydrogen. The alloys are selected in such a way that the whole cycle can be completed at the desired operating temperatures. For the average values of 230°C, 195°C, 40°C and 0°C as transformation temperature, heat source temperature, heat rejection temperature and refrigeration temperature, respectively; LaNi<sub>4.6</sub>Sn<sub>0.4</sub>, LaNi<sub>4.7</sub>Al<sub>0.3</sub> and MmNi<sub>4.15</sub>Al<sub>0.85</sub> are selected as the transformation alloy, regeneration and refrigeration alloys, respectively. These alloys are characterized with minimal plateau slope, high hydrogen capacity, less hysteresis and fast kinetics. The pressure concentration isotherms (PCI) of these

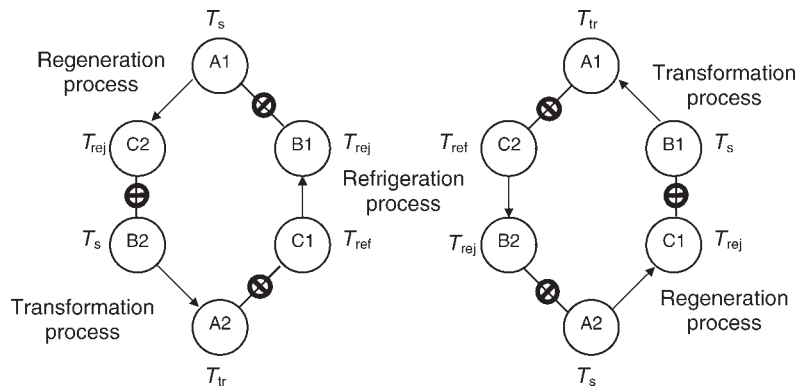


Figure 3. Schematic of the three-alloy system in six-reactor configuration.

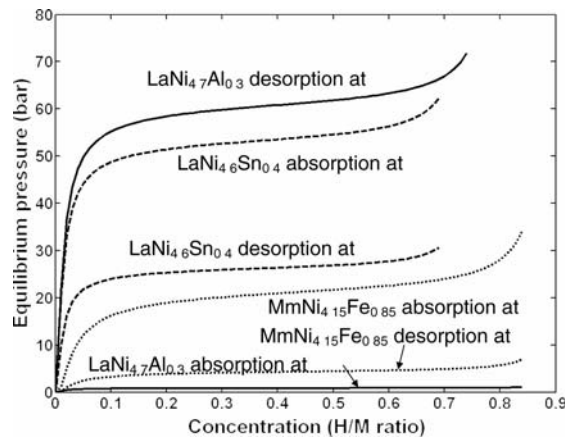


Figure 4. Pressure concentration isotherms of the alloys of the combined device for simultaneous heat transformation and refrigeration.

alloys are shown in Figure 4. These PCIs are generated using the modified van't Hoff's equation [4]

$$\ln P_{\text{eq}} = \frac{\Delta H}{RT} - \frac{\Delta S}{R} + f_s \tan\left(\pi\left(\frac{X - X_o/2}{X_o}\right)\right) + f_{\text{hys}}. \quad (1)$$

The quantity of the alloy materials is taken in such a ratio that the recyclable hydrogen capacity is the same for each alloy.

A thermal conductivity enhancement method as reported by Klein and Groll [5] has been used in the current analysis. They proposed the technique of compacting the metal hydrides using expanded natural graphite (ENG) with a metal hydride to ENG mass ratio of 14.5 and with 40% porosity. They were able to obtain thermal conductivity in the order of 30 W/mK.

## 4 PHYSICAL MODEL

Metal hydride devices are heat-driven and hence to make the devices effective, there should be efficient heat-transfer mechanisms to take away as well as to provide heat to the respective alloys without impairing the hydrogen flow between the alloys [6–10]. The physical model selected for the same is shown in Figure 5. A hollow cylindrical tube is selected for the

containment of these alloys. Hydrogen is passed to and from the tube by providing an inline porous filter through the centre of the tube. Alloys are filled in the annular space between the porous filter and tube. Heat-transfer fluid passes through the outside periphery of the tube. During a coupled reaction, hydrogen gets desorbed from one reactor absorbing heat from the heat-transfer fluid, thereby filling the central filter gas space. The pressure of hydrogen increases and this causes the other hydride to absorb it by releasing heat.

## 5 PROBLEM FORMULATION

For the prediction of the performance of the metal hydride-based thermal device, one has to model the individual reactor. One reactor will be desorbing hydrogen while the other absorbing it simultaneously. Thus for modelling the coupled reactors, heat and mass transfer equations in both the reactors are to be solved simultaneously. For the modelling of the reactions the following assumptions are made.

- (1) Metal hydrides are modelled as porous media.
- (2) Heat and mass transfer occur in the reactors in the radial direction only, i.e. the variations in the longitudinal direction are negligible and therefore the reactions are modelled in radial directions.
- (3) Heat transfer to or from the reactor occurs only through the outer periphery and that too from/to the heat-transfer fluid. There is no leakage of heat to/from the surroundings.
- (4) There is no pressure drop of hydrogen inside the hydride bed as the bed thicknesses considered are in the order of 10 mm.
- (5) Hydrogen is assumed to be an ideal gas.
- (6) The metal hydride compact does not take part in the reaction with hydrogen, but do contribute to the heat transfer.

The procedure adopted for the simulation of a coupled reaction is described below. Let the reactor that desorbs hydrogen be A and the reactor that absorbs hydrogen be B. The initial conditions of the hydrogen in the central porous filter at the start of the cycle are specified by temperature,  $T_g$  and pressure,  $P_g$ . The amount of hydrogen in the central porous filter ( $n_g$ ) is

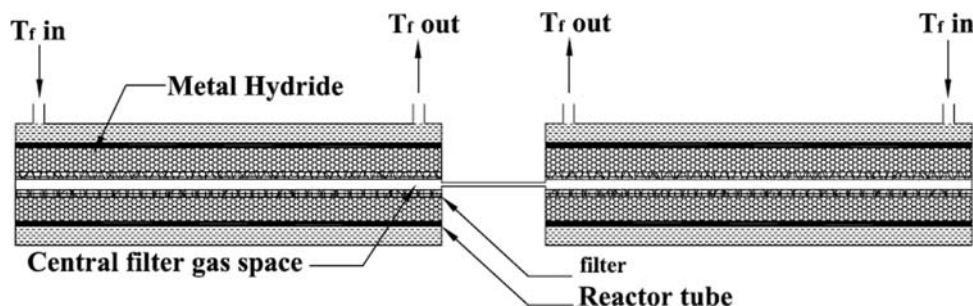


Figure 5. The physical model of a coupled reactor.

given by

$$n_g = \frac{P_g V}{RT_g} \quad (2)$$

The average temperatures of the reactors are  $T_A$  and  $T_B$ . The initial concentrations of the hydrides in the reactors A and B are  $X_A$  and  $X_B$  with  $X_A > X_B$ . The equilibrium pressures of the hydrides A and B are given by Equation (1). The equilibrium pressure of hydride A should be greater than that of the pressure in the filter gas space and similarly the equilibrium pressure of hydride B should be less than that of the hydrogen pressure in the central filter space so that hydrogen can flow from hydride A to hydride B. It is this pressure difference that drives the reaction.

The rate at which hydrogen is getting reacted is given by the reaction rate equation in terms of moles of hydrogen reacted per kilogram of alloy

$$\beta = \frac{1000 N_m dX}{2M_m dt}, \quad (3)$$

where  $dX/dt$  is the reaction kinetic equation given by [2]

$$\frac{dX}{dt} = \sigma \left( \frac{P_g - P_{eq}}{P_r} \right) \left( \frac{X - X_F}{X_I - X_F} \right) \exp \left( \frac{-E_a}{RT} \right). \quad (4)$$

Here  $P_g$  and  $P_{eq}$  denote the gas space and equilibrium pressures, respectively. In the case of absorption,  $P_g > P_{eq}$  and during desorption,  $P_g < P_{eq}$ .

The metal hydride absorption and desorption reactions are exothermic or endothermic, respectively. Therefore, as the reaction occurs temperature rises or falls in the reactor. Since the Biot number for the case under consideration is greater than one, the temperature gradients in the reactors cannot be neglected. For knowing the temperature profiles with the reaction time, transient energy balance equation has to be solved for each reactor. It is given by

$$\begin{aligned} \frac{\partial^2 T}{\partial r^2} + \frac{1}{r} \frac{\partial T}{\partial r} + \frac{\rho_{MH}(1 - \varepsilon_{MH})\beta\Delta H_f}{k_{eff}} \\ = \frac{\rho_{MHC}(1 - \varepsilon_{MHC})c_{p,MHC}}{k_{eff}} \frac{\partial T}{\partial t}. \end{aligned} \quad (5)$$

Initially, the reactors are at the temperature of the respective heat-transfer fluids. Hydride A is at fully hydrided condition and hydride B is at fully dehydrided condition. Thus the initial conditions of temperatures and concentrations for each reactor are,

$$\begin{aligned} \text{At time, } t = 0, \\ T_A(r, 0) = T_{f,A}, \quad T_B(r, 0) = T_{f,B} \\ X_A(r, 0) = X_{\max,A}, \quad X_B(r, 0) = X_{\min,B}. \end{aligned}$$

The reactors have convective heat-transfer conditions at the outside of the reactor tubes and at the inside there is no heat

transfer. So the boundary conditions are:

$$\begin{aligned} \text{at radius } r = r_i, \quad dT/dr = 0, \\ \text{at radius } r = r_o \\ -k_{eff} \frac{dT}{dr} = h(T(r_o, t) - T_f). \end{aligned}$$

## 6 SOLUTION METHODOLOGY

The energy balance Equation (5) is solved for both the reactors for temperatures and concentration in space and time. The equation is discretized according to the Crank Nicolson Algorithm and the resulting algebraic equations were solved using the Thomas Algorithm TDMA solver.

The number of moles of hydrogen reacted in each reactor for each time step is computed using the equation

$$n = \Delta t \times \int_{r_i}^{r_o} 2\pi r l \rho_m (1 - \varepsilon) \beta dr. \quad (6)$$

Using the amount of hydrogen reacted in each reactor for each time step, the amount of hydrogen in the central porous filter for the new time is found out (old mass + mass desorbed – mass absorbed). The new temperature is found out by doing energy balance for hydrogen in the central porous filter. The new pressure in the gas space is found out using the ideal gas equation using the new mass and temperature. This pressure is used for the estimation of the reactions for the next time step.

The amount of heat exchanged with heat-transfer fluid for each time step is found out using the relation

$$Q = 2\pi r_o l h (T(r_o, t) - T_f) \times \Delta t. \quad (7)$$

The above procedure is continued with time till the prescribed time for a particular process is reached. Simulation is done for the three processes by which a cycle is completed. The simulation of several consecutive cycles is done till the properties of all the hydrides and hydrogen for consecutive cycles are identical.

Performance of the system is defined using the parameters of  $COP_{ref}$  and specific cooling potential (SCP) for cooling. Similarly, in the case of heat transformation, the performance is defined using  $COP_{tr}$  and specific amplification potential (SAP). These parameters are defined as follows:

$$COP_{ref} = \frac{\text{Net cooling effect at refrigeration temperature}}{\text{Net heat input at source temperature}}, \quad (8)$$

$$SCP = \frac{\text{Net cooling effect}}{\text{Cycle time} \times \text{Total mass of hydrides}}, \quad (9)$$

$$\begin{aligned} COP_{tr} \\ = \frac{\text{Net transformation output at transformation temperature}}{\text{Net heat input at source temperature}}, \end{aligned} \quad (10)$$

$$SAP = \frac{\text{Net transformation output}}{\text{Cycle time} \times \text{Total mass of hydrides}} \quad (11)$$

## 7 RESULTS AND DISCUSSION

As mentioned earlier, the study is done for the case where six reactors of three alloys are coupled with each other. All the three processes occur at the same time so that all the six reactors take part in the reactions at any given time. The cycle consists of two steps and each reactor goes through a hydrogen

absorption–desorption cycle. For the sake of simplicity it is assumed that each of the three processes is of the same duration. The simulation is done for the case of three reactors, as essentially the COP remains the same as that of the six-reactor system and the SCP and SAP are 1.5 times of that of the three-bed system. Thus the simulation is performed for the three-bed system with equal process times and the results are extended for the case of the six-reactor system.

### Temperature and concentration profiles

Figures 6 and 7 show the temperature and concentration profiles of the three-reactor system during the operation of a cycle.

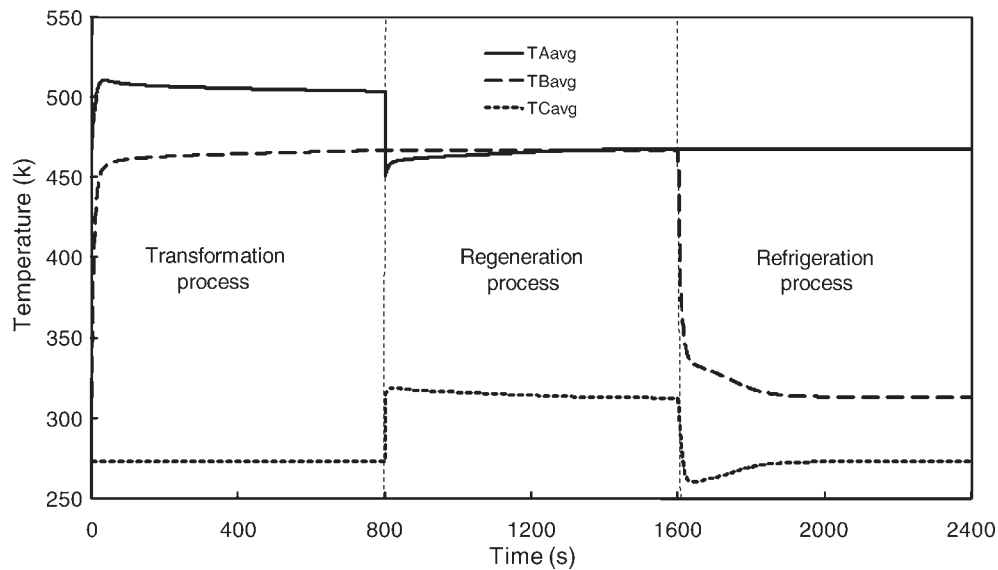


Figure 6. Variation of temperature profiles for the three hydrides in a cycle for a process time of 800 s.

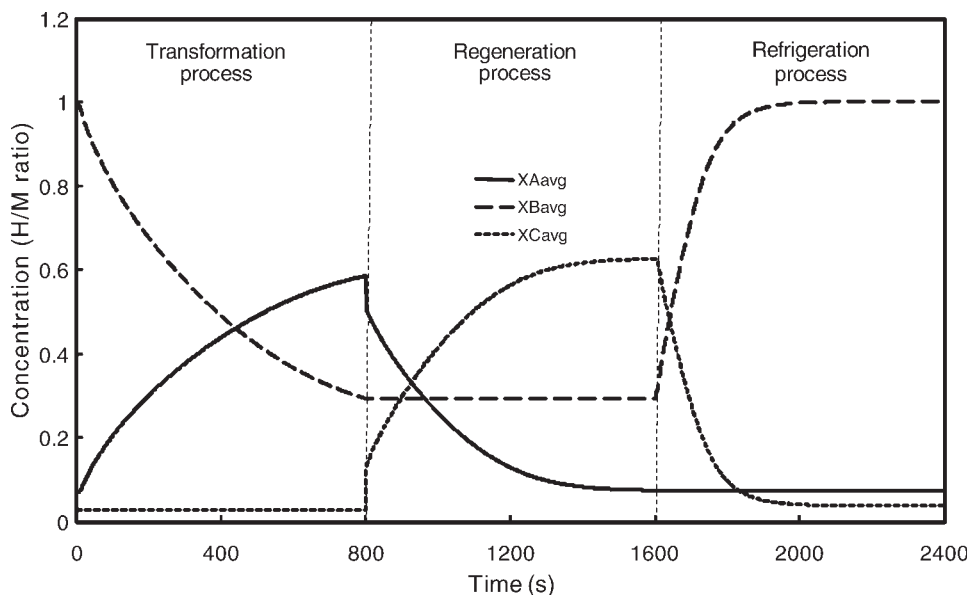


Figure 7. Variation of concentration profiles for the three hydrides in a cycle for a process time of 800 s.



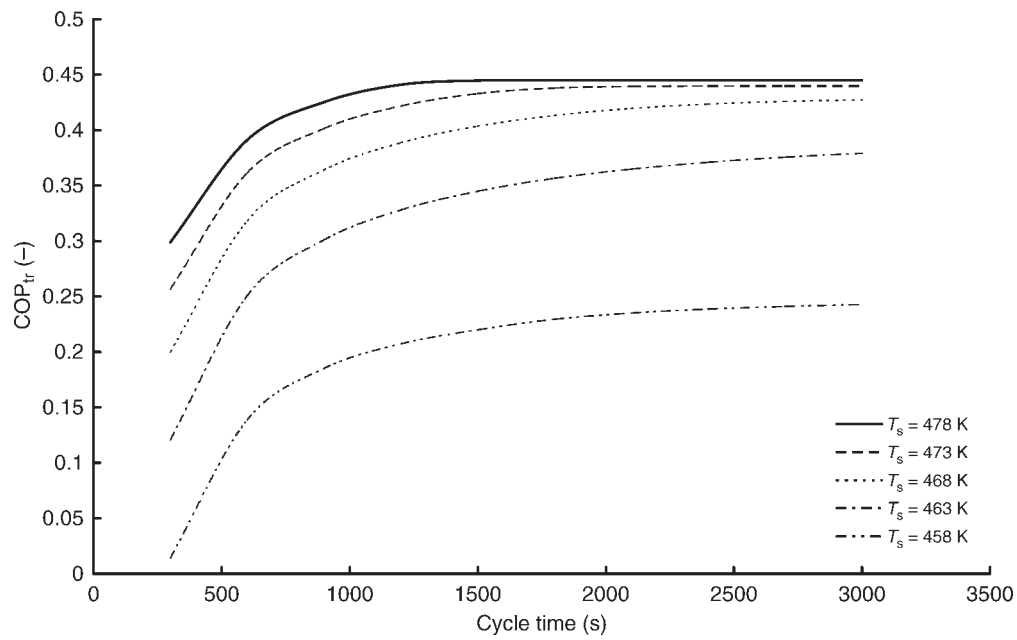


Figure 8. The effect of the variation of cycle time on the transformation COP for various heat source temperatures.

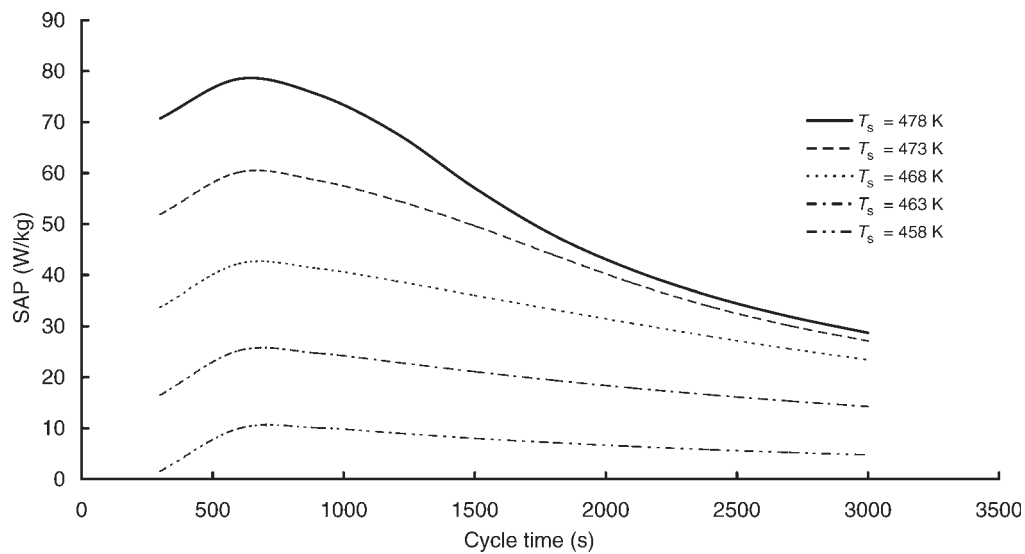


Figure 9. The effect of the variation of cycle time on the SAP for various heat source temperatures.

The profiles can be seen for the three different processes of transformation, regeneration and refrigeration for each of the metal hydrides, A, B and C. The time for each process in the depicted case is 800 s. In the transformation process metal hydride B desorbs hydrogen taking heat from heat source and the same is absorbed by metal hydride A releasing the heat of transformation. Since hydride C does not take part in the transformation process, the profiles for hydride C are invariant. The variation of concentration for the hydrides can be seen from Figure 7. Average concentration of hydride A increases, whereas that of hydride B decreases with time in the transformation process. Similar trends can be observed in the

regeneration and refrigeration processes. Although the temperatures of hydrides reach the respective heat-transfer fluid temperature well before the whole time of the process, the concentrations have not reached its limits. The rate of change of concentration is less during the latter part of the reaction, resulting in a lesser heat transfer to the fluid. Since the transformation and refrigeration outputs are obtained from the heat-transfer fluids there is a possibility of improving the specific output of transformation (SAP) and refrigeration (SCP) by optimizing the process times. The effect of variation of process times are considered in the subsequent section.

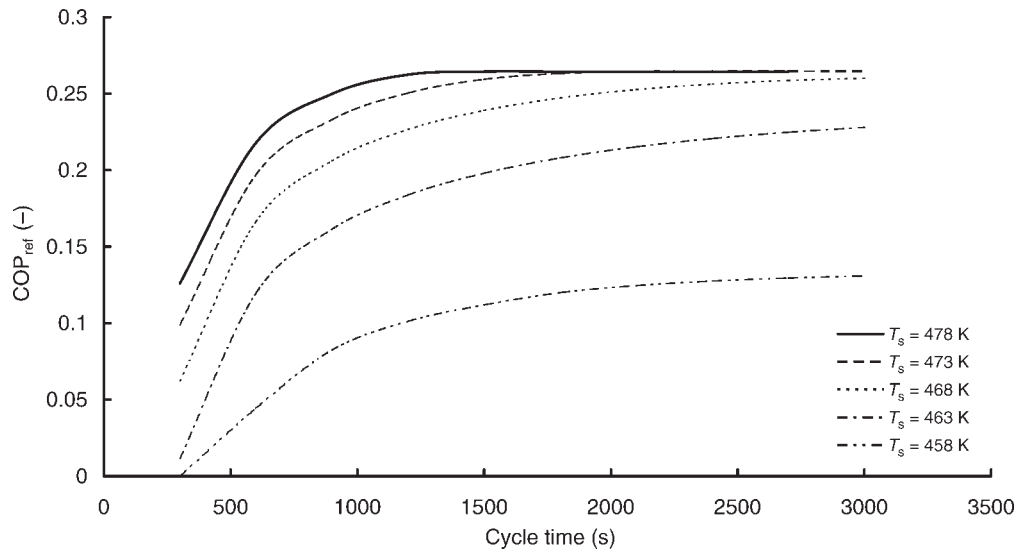


Figure 10. The effect of the variation of cycle time on the refrigeration COP for various heat source temperatures.

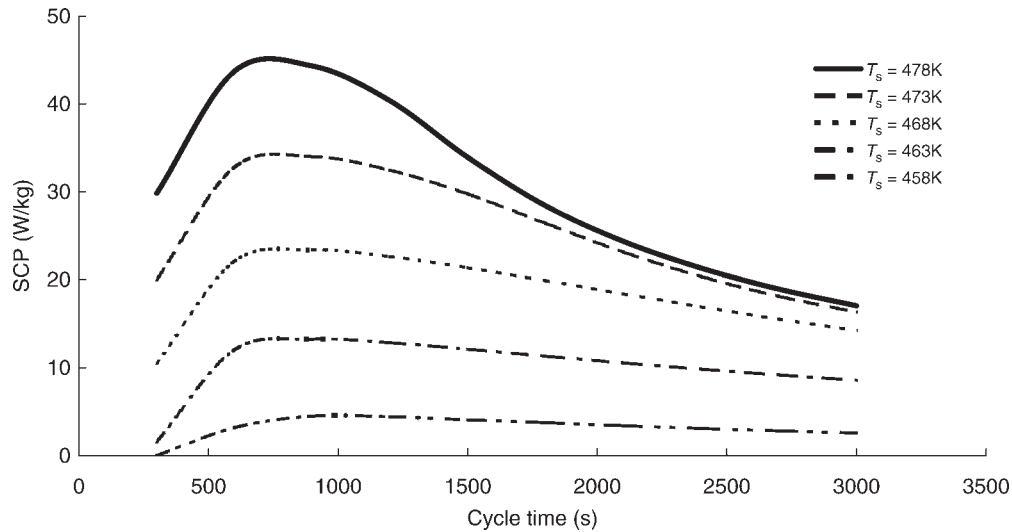


Figure 11. The effect of the variation of cycle time on SCP for various heat source temperatures.

### Variation of transformation and refrigeration outputs with process time

For finding the impact of process times on the system performance, the process times of each process are varied in steps of 100 s, from 100 s to 1000 s, thereby obtaining a cycle time of 300–3000 s. The effect of heat source temperature ( $T_s$ ) on the output was found by its variation. All other parameters are kept constant. The transformation output is expressed as  $COP_{tr}$  and SAP, whereas refrigeration output is expressed as  $COP_{ref}$  and SCP. The results obtained for the same are shown in Figures 8–11.

It can be seen from Figure 8 that  $COP_{tr}$  increases with the increase of cycle time and becomes constant. The same behaviour is observed for all heat source temperatures. The transformation alloy, A, has to be brought up to the transformation

temperature ( $T_{tr}$ ) from the previous regeneration process temperature ( $T_s$ ) in which A is earlier. Hence in the initial times of the transformation process, most of the heat of transformation is expended for the sensible heating of the alloy from  $T_s$  to  $T_{tr}$  and thereby the transformation output will be negligible in the initial times. This is the reason for the decreased  $COP_{tr}$  in the case of smaller process times.  $COP_{tr}$  increases till the increase in transformation output and it attains a constant value once the transformation process is over, beyond which the increase of process time does not show any effect. Keeping a process time in the case where the COP has already stabilized is not justified. It can be observed that the effect of sensible heating of the alloys cannot be neglected in the working of the system. It can be seen that the  $COP_{tr}$  increases with the increase of heat source temperature. This is

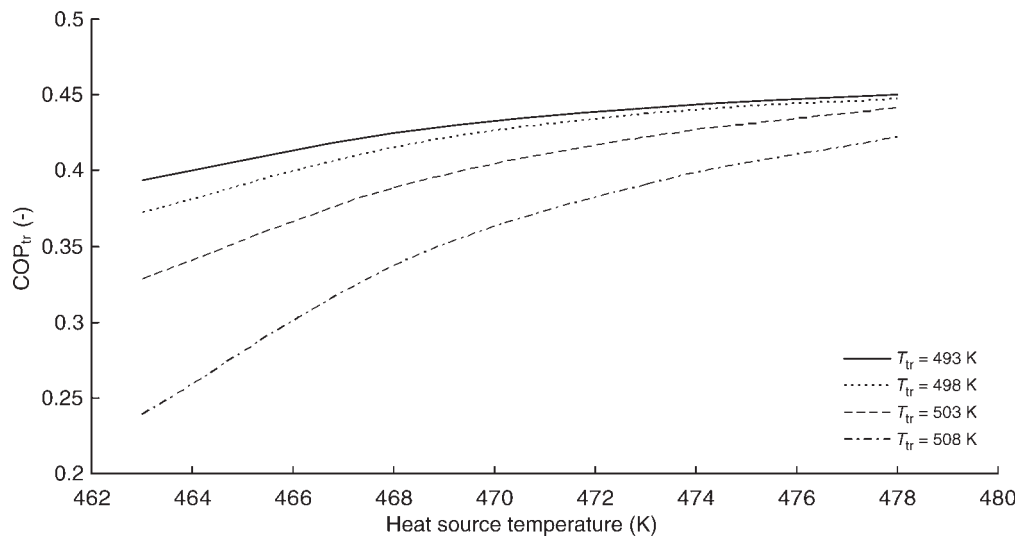


Figure 12. The effect of the variation of transformation temperature on the transformation of COP for various heat source temperatures.

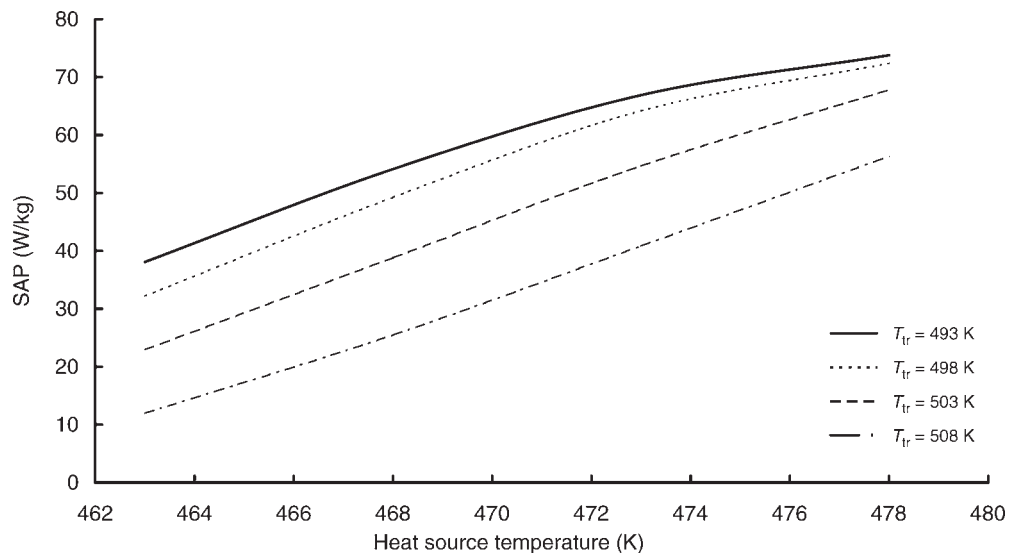


Figure 13. The effect of the variation of transformation temperature on SAP for various heat source temperatures.

because of the larger transformation output obtained because of the increase of source temperature. Similar characteristics as that of  $COP_{tr}$  are obtained for  $COP_{ref}$  as seen in Figure 10. Here the decrease in  $COP_{ref}$  for the lesser cycle times is owing to the sensible cooling of the refrigeration alloy, C, from  $T_{rej}$  to  $T_{ref}$ . The effect of increase of COP with the increase of heat source temperature is seen in the case of refrigeration output also. Although the heat source temperature does not have a direct relation with the refrigeration process, since all the processes are influenced by each other, the better performance of the transformation process causes more hydrogen to get reacted and it facilitates the better performance of the refrigeration process because of the excessive availability of hydrogen.

The variation of SAP and SCP with respect to cycle times and heat source temperatures is shown in Figures 9 and 11. These profiles show the rate at which the transformation and refrigeration output are obtained. It can be seen that the rate of output increases initially, reaches a maximum and decreases with the increase in the cycle time. From the figure it is noticeable that there exists an optimum cycle time for which the best rate of output can be obtained. If the SAP and SCP profiles are matched with the  $COP_{tr}$  and  $COP_{ref}$  profiles, it can be noticed that the cycle times for which the maximum output rates are obtained, the COP is about 90% of the maximum COP obtained. The SAP and SCP profiles can serve as a guide in deciding the cycle time for a system and by this way the highest output for a given time span can be obtained.



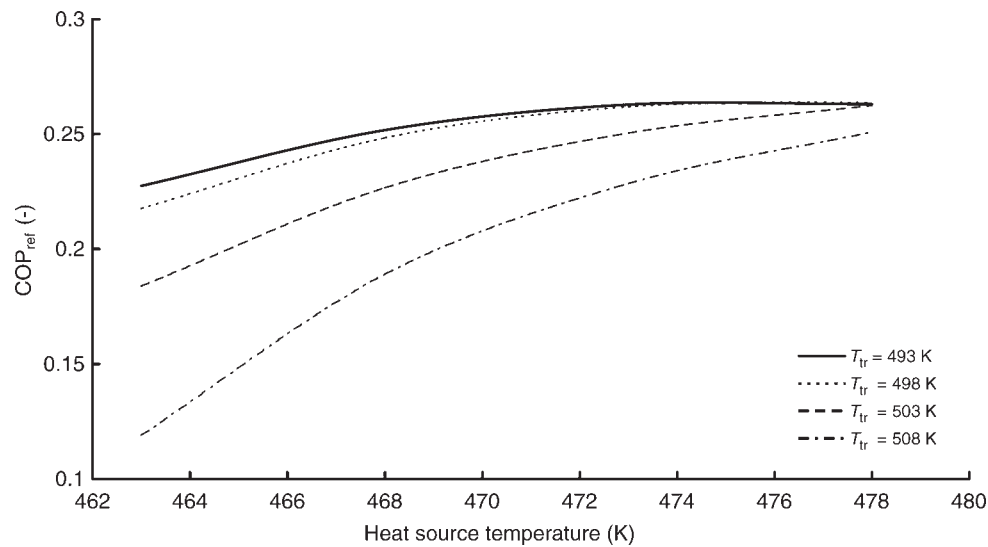


Figure 14. The effect of the variation of transformation temperature on the refrigeration of COP for various heat source temperatures.

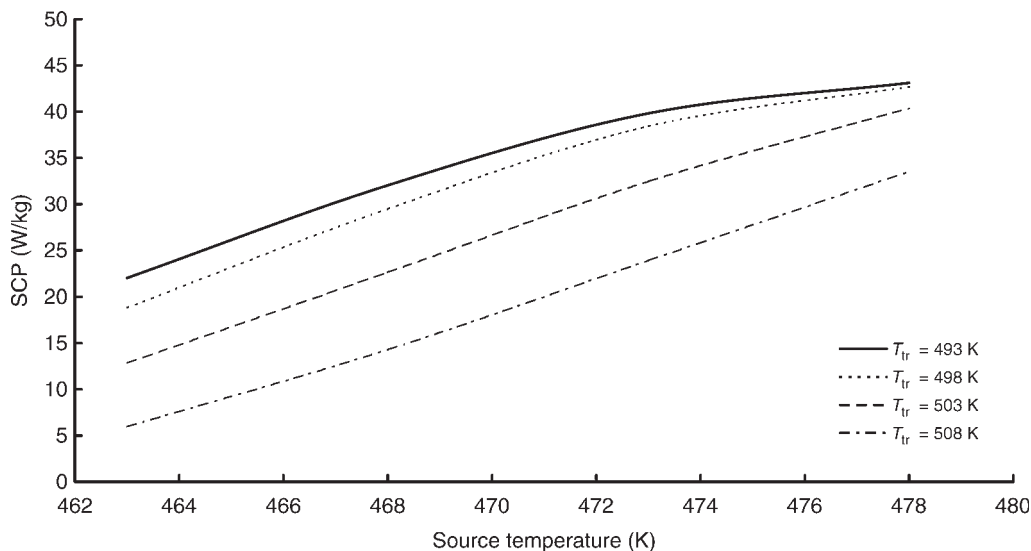


Figure 15. The effect of the variation of transformation temperature on SCP for various heat source temperatures.

### Variation of transformation and refrigeration outputs with operating temperatures

For analysing the effect of operating temperatures on the system performance, the transformation and refrigeration temperatures were varied for various heat source temperatures. The system performance is studied by analysing the effect on COPs, SAP and SCP. The effect of different transformation temperatures are shown in Figures 12–15.

From the figures, the common aspect that can be observed is that the system performance increases with the increase of heat source temperature and with the decrease of heat transformation temperature. This can be explained based on the PCI characteristics of the metal hydrides. The driving potential for the heat-transformation process is the difference in

equilibrium pressure difference of heat-transformation alloy, A at  $T_{tr}$  and that of B, at  $T_s$ . As the heat-transformation temperature reduces and as the heat source temperature increases, the potential increases. This causes an increase in the rate of the transformation reaction and for more hydrogen to get reacted and thereby for a better performance of each of the processes.

Another observation found is that the profiles for SAP and SCP show a linear behaviour, whereas the profiles for COPs show a nonlinear behaviour. The rate of increase of COP is more at lesser heat source temperatures. The COP is defined as the ratio of output to input and the variation of temperature has a compound effect on it. In the case of increase of heat source temperature, the transformation output increases and at the same time the input also increases. At higher heat source

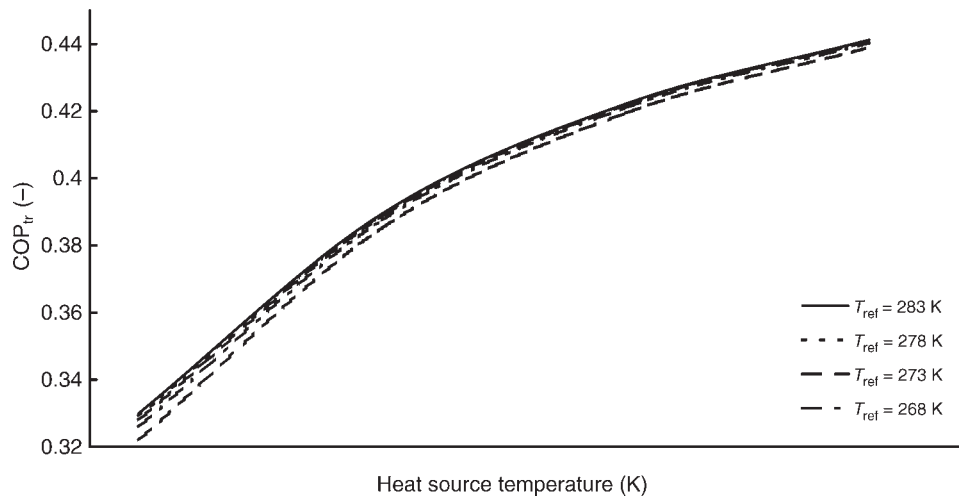


Figure 16. The effect of the variation of refrigeration temperature on the transformation of COP for various heat source temperatures.

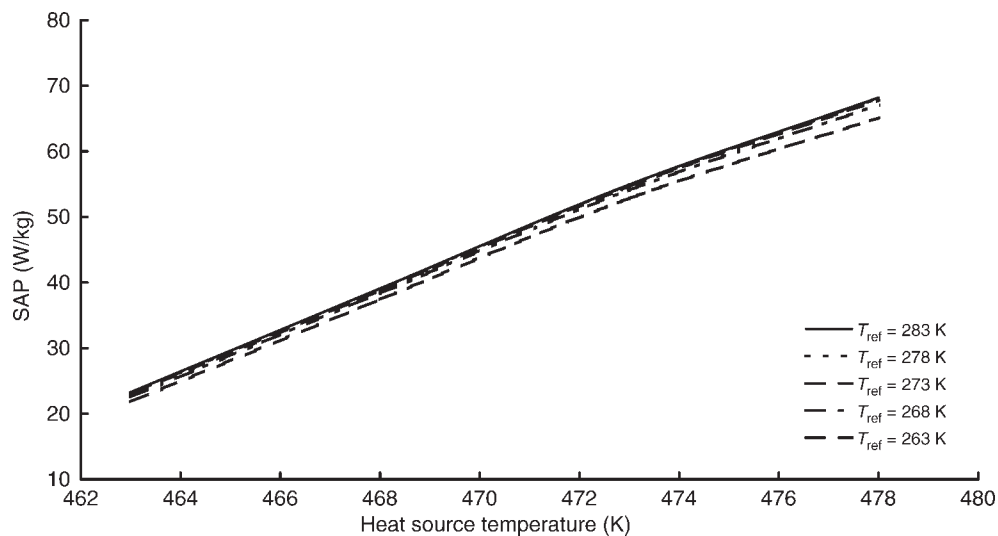


Figure 17. The effect of the variation of refrigeration temperature on SAP for various heat source temperatures.

temperatures, the increase in the input is more pronounced than the increase in the output and this causes a lesser rate of increase of COP. Since the SAP and SAP are functions of output alone it more or less shows a linear relationship with the variation of temperature.

The effect of the variation of refrigeration temperature on the transformation and refrigeration output performance is shown in Figures 16–19. In this case both the transformation and refrigeration outputs are increasing with the increase in refrigeration temperature. It can be seen that the effect of variation on the transformation is negligible when compared with the effect on refrigeration. The variation of refrigeration temperature for alloy, C does not appreciably change the amount of hydrogen reacted because the change in equilibrium pressure for alloy C with refrigeration temperature is negligible. Since the hydrogen reacted does not change significantly, there is no

effect on the transformation process. The effect seen on the refrigeration process is due to the increase of sensible cooling required with the reduction of refrigeration temperature.

From the observation of the results obtained for the variation of operating temperatures, it can be concluded that it is the intrinsic properties of the metal hydrides at corresponding temperatures, which decides the performance of these systems.

## 8 CONCLUSIONS

A heat and mass transfer study of a metal hydride device working with three different alloys for simultaneous heat transformation and refrigeration has been conducted. Simulation of the working of the system with actual reactor configurations and with all the three alloys in unison was performed.

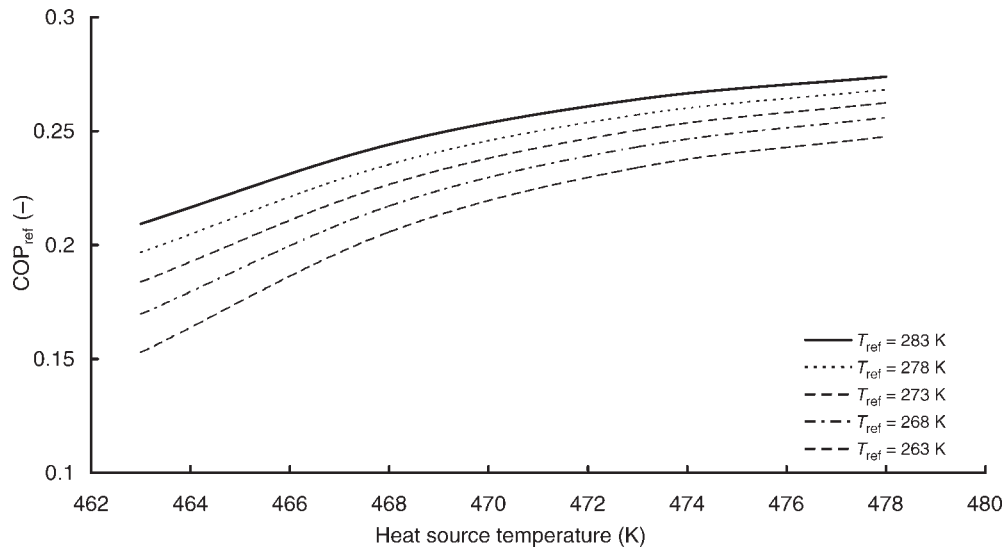


Figure 18. The effect of the variation of refrigeration temperature on the refrigeration of COP for various heat source temperatures.

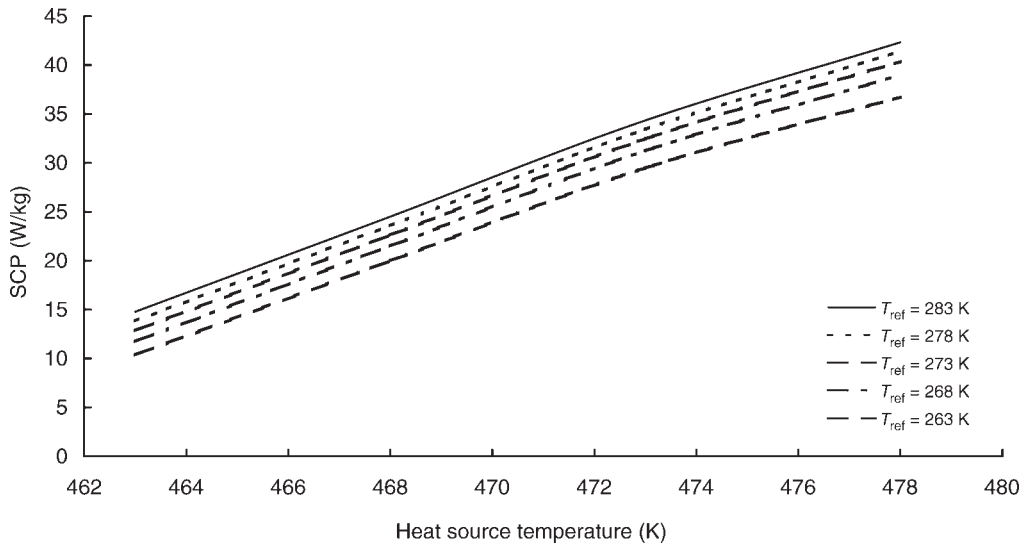


Figure 19. The effect of the variation of refrigeration temperature on SCP for various heat source temperatures.

The effect of cycle time and operating temperatures on the performance of the system was conducted. The following conclusions were made based on the study.

- (1) As shown in the results for the proper understanding of the working of metal hydride devices, heat and mass transfer study is essential.
- (2) Better rate of transformation and refrigeration output can be obtained by the optimization of cycle times and this aids in maximizing the energy output for a particular span of time.
- (3) The better performance of any single process in a cycle will help in the better performance of other processes also in the cycle and vice versa.
- (4) The inherent properties of metal hydrides play a major role in the performance of these systems and the variation

of the performance with the variation temperatures happens predominantly because of these.

- (5) The effect of sensible heating and cooling has an effect on the system performance and it has to be ensured that the sensible heat component to be maintained at a minimum.

## NOMENCLATURE

$c_p$	specific heat capacity (J/(kgK));
$E_a$	activation energy (J/mol);
$f_{hys}$	hysteresis factor;
$f_s$	slope factor;
$\Delta H$	enthalpy of formation (kJ/(mol H <sub>2</sub> ));
H/M	hydrogen to metal atomic ratio;

$h$	overall heat transfer coefficient (W/(m <sup>2</sup> K));
$k_{\text{eff}}$	effective thermal conductivity (W/(mK));
$l$	length of reactor (m);
$M_m$	molecular weight of alloy (g/mol);
$N_m$	number of atoms per molecule of alloy;
$n$	moles of hydrogen;
$P$	pressure (bar);
$R$	Universal gas constant (J/(molK));
$r$	radius (m);
$\Delta S$	entropy of formation (kJ/(mol H <sub>2</sub> ));
$T$	temperature (K);
$t$	time (s);
$V$	volume of gas space (m <sup>3</sup> );
$X$	concentration (H/M ratio);
$X_o$	maximum concentration limit;
$\beta$	reaction rate, mole of H <sub>2</sub> /kg of alloy;
$\varepsilon$	porosity;
$\rho_m$	density of metal (kg/m <sup>3</sup> );
$\sigma$	reaction rate constant (1/s)

## Subscripts

A	MH A;
B	MH B;
eq	equilibrium;
F	final;
f	fluid;
g	gas;
h	high;
I	initial;
i	inner;

l	low;
MH	metal hydride;
MHC	metal hydride compact;
m	medium;
max	maximum;
min	minimum;
o	outer

## REFERENCES

- [1] Ram Gopal M, Srinivasa Murthy S. Prediction of metal-hydride refrigerator performance based on reactor heat and mass transfer. *Int J Hydrogen Energy* 1995;20:607–14.
- [2] Kang BH, Kuznetsov A. Thermal modelling and analysis of a metal hydride chiller for air conditioning. *Int J Hydrogen Energy* 1995;20:665–74.
- [3] Ahmed SS, Srinivasa Murthy S. Analysis of a novel metal hydride cycle for simultaneous heating and cooling. *Renew Energy* 2004;29:615–31.
- [4] Nishizaki T, Miyamoto K, Yoshida K. Coefficients of performance of hydride heat pumps. *J Less Common Metals* 1983;89:559–66.
- [5] Klein HP, Groll M. Heat transfer characteristics of expanded graphite matrices in metal hydride beds. *Int J Hydrogen Energy* 2004;29:1503–11.
- [6] Dantzer P, Orgaz E. Thermodynamics of hydride chemical heat pump—II. How to select a pair of alloys. *Int J Hydrogen Energy* 1986;11:797–806
- [7] Sun DW, Deng SJ. Study of the heat and mass transfer characteristics of metal hydride beds. *J Less Common Metals* 1988;141:37–43
- [8] Choi H, Mills AF. Heat and mass transfer in metal hydride beds for heat pump applications. *Int J Heat Mass Transfer* 1990;33:1281–8
- [9] Ram Gopal M, Srinivasa Murthy S. Performance of a metal hydride cooling system. *Int J Refrig* 1995;18:413–20
- [10] Fedorov EM, Shanin YI, Izhvanov LA. Simulation of hydride heat pump operation. *Int J Hydrogen Energy* 1999;24:1027–32